Application of sludge-based carbonaceous materials in a hybrid water treatment process based on adsorption and catalytic wet air oxidation

Carine Julcour Lebigue [a,*], Caroline Andriantsiferana [a], N'Guessan Krou [a], Catherine Ayral [a], Elham Mohamed [a], Anne-Marie Wilhelm [a,†], Henri Delmas [a], Laurence Le Coq [b], Claire Gerente [b], Karl M. Smith [c], Suangusa Pullket [c], Geoffrey D. Fowler [c], Nigel J.D. Graham [c]

[a] Université de Toulouse, Laboratoire de Génie Chimique, UMR CNRS 5503, 4, allée Emile Monso, BP 84234, 31432 Toulouse Cedex 4, France
[b] GEPEA UMR 6144, Ecole des Mines de Nantes, 4 rue Alfred Kastler, 44307 Nantes Cedex 3, France
[c] Department of Civil and Environmental Engineering, Imperial College London, South Kensington Campus, London SW7 2AZ, UK

A B S T R A C T

This paper describes a preliminary evaluation of the performance of carbonaceous materials prepared from sewage sludges (SBCMs) in a hybrid water treatment process based on adsorption and catalytic wet air oxidation; phenol was used as the model pollutant. Three different sewage sludges were treated by either carbonisation or steam activation, and the physico-chemical properties of the resultant carbonaceous materials (e.g. hardness, BET surface area, ash and elemental content, surface chemistry) were evaluated and compared with a commercial reference activated carbon (PICA F22). The adsorption capacity for phenol of the SBCMs was greater than suggested by their BET surface area, but less than F22; a steam activated, dewatered raw sludge (SA_DRAW) had the greatest adsorption capacity of the SBCMs in the investigated range of concentrations (<0.05 mol L^{-1}). In batch oxidation tests, the SBCMs demonstrated catalytic behaviour arising from their substrate adsorptivity and metal content. Recycling of SA_DRAW in successive oxidations led to significant structural attrition and a hardened SA_DRAW was evaluated, but found to be unsatisfactory during the oxidation step. In a combined adsorption–oxidation sequence, both the PICA carbon and a selected SBCM showed deterioration in phenol adsorption after oxidative regeneration, but a steady state performance was reached after 2 or 3 cycles.

1. Introduction

Sludge arising from waste water treatment has become a critical environmental issue due to growing water demands and more stringent water quality standards. From 5.5 million tonnes of dry matter in 1992 the production of sludge in the European Union has increased to about 9 million tonnes in 2005 (European Commission, 2010). Landspreading, agricultural use and incineration remain the major disposal outlets for sewage sludge. However, the former solutions have to deal with low societal acceptance and severe requirements to avoid accumulation of toxic compounds in soils and vegetation, while incineration suffers from poor sustainability.

As part of the recent European research project, REMOVALS (FP6-018525), concerned with identifying alternative solutions for better disposal and reuse of waste sludge, a collaborative study has been developed between Imperial College (London), GEPEA (Nantes) and LGC (Toulouse) for the production of activated carbons from sewage sludge and their use in a sequential water treatment process involving both adsorption and catalytic wet air oxidation (CWAO).

In this adsorption–oxidation (AD–OX) process, water treatment was realised at ambient conditions by adsorption on activated carbon (AC), and subsequent batch wet air oxidation at higher temperature and pressure on the same bed of AC to destroy the adsorbed organic pollutants and regenerate the carbon in-situ for further adsorption (Delmas et al., 2002, 2009). This second step can be performed in mild conditions (typically 150 °C and 20 bar of air) as activated carbons have been found to promote the liquid phase oxidation of several organic compounds, in particular phenols (Fortuny et al., 1998; Suarez-Ojeda et al., 2005; Santos et al., 2005; Creanga Manole et al., 2007).

The application of sludge-based materials has been successfully reported for the uptake of metal ions (Rio et al., 2005; Seredych and Bandosz, 2006; Martin et al., 2002), dyes (Martin et al., 2002; Otero et al., 2003; Rio et al., 2005; Rozada et al., 2007; Fan and Zhang,

* Corresponding author. Tel.: +33 5 34 32 37 09; fax: +33 5 34 32 37 00.
E-mail address: carine.julcour@ensiacet.fr (C. Julcour Lebigue).
† Deceased on 1st June 2009.

2008), and phenolic compounds (Otero et al., 2003; Rio et al., 2005). For the proposed application, the synthesised materials should combine both good adsorption capacities for the organic pollutants and effective catalytic properties for their oxidation, as well as high attrition resistance. In particular, the substantial amount of inorganic matter found in carbons prepared from physical activation of sludges is usually detrimental for adsorption as it results in low BET surface area materials, but it could be beneficial for their regeneration if active transition metals like iron or copper are present as observed with metal impregnated carbons (Matatov-Meytal and Sheintuch, 1997; Quintanilla et al., 2006). Moreover the relatively high mesoporosity of sludge-based carbonaceous materials (SBCMs) can also be of interest as condensation products formed during the CWAO of phenols on AC are capable of blocking the micropores (Cordero et al., 2008).

In our study reported here, six different carbonaceous materials prepared from the carbonisation of municipal WWTP sludges with or without physical activation were fully characterised and compared according to the aforementioned criteria: adsorption capacity for phenol, catalytic activity and stability for the CWAO of the pollutant, and finally, use in the sequential AD–OX process. A commercial carbon (PICA F22) was also used in this study as a reference material.

2. Production and characterisation of SBCMs

2.1. Production

Three different sewage sludges have been used as feedstock for production of the carbons: DMAD (dewatered, mesophilic anaerobically digested), DRAW (dewatered, raw) and DSBS (dewatered, secondary biological). DSBS was collected in a municipal WWTP in Nantes, whereas DMAD and DRAW originated from the UK (Ashford and Little Marlow respectively). The composition of these parent sludges is given in Table 1. The volatile content of the sludge samples was determined using a Thermal Analyser (PL Thermal Sciences STA1500). 10–15 mg specimens of each dried sludge sample were heated at 5 °C/min under nitrogen from room temperature to 1000 °C. The volatile content on a moisture-free basis was calculated from the percentage loss in weight of the sample incurred by heating it from 150 °C to 850 °C, with the weight of the sample at 150 °C being used as the baseline (dry) weight of the sample.

From the UK sludges, both charred and steam activated samples were prepared. Prior to carbonisation, the sludges were sterilised, dried to constant mass at 105–110 °C and finally ground below 10 mm in size. Subsequently, *ca.* 210 g of sample were loaded into a quartz reactor, which was then installed within a Carbolite rotary furnace (model HTR11/150). They were heated at 5 or 10 °C min^{-1} under a flowing (500 mL min^{-1}) nitrogen atmosphere. After the desired temperature (from 250 to 1000 °C) was reached, the furnace was automatically cooled down to produce carbonised samples. When steam activation was applied, the only difference was that once the target temperature was reached, the equivalent of 0.7 g min^{-1} of steam was mixed with the nitrogen flow (acting as carrier) and the temperature was maintained for the whole duration of the prescribed activation period. The flow of the activation reagent was arrested and the furnace was left to cool at the end of the activation period.

A carbonisation temperature of 900 °C achieved an optimal BET and microporous surface area of the carbon series. The steam activation procedure was optimised using the response surface methodology (Karacan et al., 2007) to establish the relationship between the textural properties of the resulting carbonaceous materials and the applied conditions. From the models it was calculated that the maximum BET surface area was attained when the activation temperature was 838 °C and dwell time was 80 and 73 min for DRAW and DMAD based carbons, respectively (Pullket et al., 2009). These similar conditions of activation indicate that the post-carbonisation carbon component of the two sludges is essentially the same. Thus four samples were synthesised from the two sludges using these optimal conditions of carbonisation and steam activation, respectively.

The DSBS sludge underwent a different activation procedure, conducted with CO_2: the sample was first carbonised at 600 °C for 1 h under 2 L min^{-1} of N_2; then the temperature was increased to an optimum activation temperature of 875 °C and the gas flow was switched to CO_2 (1.5 L min^{-1}) for one more hour.

In this paper the carbonised series of carbons are referred to as "C_DMAD" or "C_DRAW" according to the sludge origin, while steam activated samples are labelled with the prefix "SA_" and the CO_2 activated DSBS is addressed as "CA_ DSBS".

The F22 commercial AC, used as reference, was provided by PICA (VEOLIA group) and was made from coal.

All carbons have been subsequently characterised in detail in order to identify the key physico-chemical properties that may explain their behaviour in the AD–OX process and thus aid in the design of optimal SBCMs for this specific application.

2.2. Physico-chemical properties of SBCMs

2.2.1. Textural properties

2.2.1.1. Ball pan hardness. As a good attrition resistance of the SBCMs is a key issue for their use in high pressure fixed bed reactors (especially with cocurrent gas–liquid upflow), the hardness of the sludge-based carbons has been measured. A modified form of the ASTM ball pan hardness method (ASTM D3802) was used for this purpose, where 50 cm^3 of the carbons, sieved between 0.5 and 2 mm, was put into a 8″ (200 mm) receiver adapted to the specifications stipulated by the ASTM method. To this, 15 large steel balls and 15 small steel balls, measuring 13 mm and 9.5 mm in diameter respectively, were added and the resulting assembly was shaken for 30 s using an Endecotts Octagon Digital sieve shaker (London, UK). The weight percentage of the original sample which was not crushed below 0.5 mm in size by attrition defined the hardness number.

After calibration with a commercial carbon (Filtrasorb 400 (Chemviron, Ashton-in-Makerfield, UK)) with a known hardness number (≈95%), the method was applied to the SBCMs. For the DSBS and DMAD based carbons values comparable to those obtained with commercial ACs were measured (>95%), while the DRAW based carbons were friable with a hardness number in the range of 57–71% (the hardness is influenced by the carbonisation/steam activation conditions used). An additional batch of SA_DRAW particles was prepared by pelletisation of the milled steam activated sludge together with a binder (PVA, 5 wt%), which resulted in a hardness number of 92–93%.

2.2.1.2. Textural properties. The nitrogen adsorption/desorption isotherms were measured at 77 K with a Micromeritics ASAP 2010 surface area analyser. The specific surface area was calculated from a BET plot for relative pressures between 0.01 and 0.2 (Brunauer

Table 1
Composition of the parent sludges.

Sludge	C (wt%)[a]	Ash (wt%)[a]	Volatile content (wt%)
DMAD	32.1	39.6	53.4
DRAW	41.0	20.4	65.9
DSBS	40.3	23.6	68.2

[a] From Pullket et al. (2009).

et al., 1938), whereas the mesoporous and microporous volumes were estimated according to Barrett et al. (1951) and Horvath and Kawazoe (1983) theories, respectively. The mean pore diameter was deduced from the total porous volume at $p/p_0 = 0.98$ and the BET surface area.

The structural density of the materials was also measured from helium pycnometry (AccuPyc 1330TC).

The porosity, ratio of pore to particle volume, was then calculated from the total porous volume V_p and structural density ρ_S according to:

$$\varepsilon_p = \frac{V_p}{V_p + \frac{1}{\rho_S}} \quad (1)$$

The corresponding values are reported in Table 2.

The BET surface area of the sludge-based carbons was rather modest, four to ten times lower than that of the commercial AC. As expected steam activation improved the textural properties of the materials, but the differences appeared to mainly result from the various sludge sources.

Introduction of the hardening binder slightly reduced the surface area of SA_DRAW, yielding a good compromise in comparison to the other hard sludge-based carbons.

The porosity of the SBCMs was well distributed between micro- and mesopores, while F22 exhibited much more microporosity.

2.2.2. Global chemical analyses

2.2.2.1. Elemental analysis and ash content. Elemental analysis of the ACs was carried out using a Thermo Finnigan Flash EA111 for CHNSO determination and acid lixiviation ($HCl:HNO_3 = 3:1$ v/v) followed by inductively coupled plasma atomic emission spectroscopy (Jobin Yvon – Ultima 2R) for metals. Metals whose oxides could act as oxidation catalysts were investigated.

The ash content was determined by calcination at 650 °C until constant weight according to ASTM D2866 (1995).

The results of the chemical analyses are given in Tables 3 and 4.

Table 4 reveals a very high ash content in SBCMs which is consistent with the literature on the preparation of SBCMs by carbonisation and steam activation (Smith et al., 2009). The ash content is about 10% higher for DMAD based materials as compared to DRAW ones, which is consistent with their lower BET surface area and the lower carbon content of their parent sludge. During digestion the less recalcitrant organic molecules of the DMAD sludge have been converted into gases, leaving a higher proportion of inorganic matter. Conversely the high carbon content of the DSBS has surprisingly not yielded a larger surface area. It could be due to the different precursor material or to the activation method employed, using CO_2, which is a slower process than steam activation.

The SBCMs from UK sludges are also characterised by a large amount of iron, about 100 times more than in the commercial AC.

Finally, it can be seen that the SBCMs contained a rather high percentage of oxygen (Table 3), which can be related to the presence of surface functional groups and, at a greater degree, to inorganic salts and oxides.

Table 3
CHNSO elemental analysis of physically activated SBCMs and F22.

Carbon	C (wt%)	H (wt%)	N (wt%)	S (wt%)	O (wt%)
SA_DMAD	22.6	0.6	< 0.1	nd	6.1
SA_DRAW	27.9	0.6	1.4	0.8	10.3
CA_DSBS	34.2	0.6	2.7	nd	10.5
PICA F22	84.4	0.5	0.5	0.7	1.1

2.2.2.2. SEM/EDX analysis. A complementary chemical analysis was conducted on SBCMs using an Energy Dispersive X-ray microprobe (INCA system, Oxford Instrument) operated in tandem with a Scanning Electron Microscope (LEO 435 VP). Contrary to the previous methods, it provides principally a surface analysis of the samples due to the low penetration depth of the incident electrons (about 1 μm), and it is sensitive to surface defects (roughness, pores) and heterogeneity of the powder particles.

The following conditions were applied: working distance = 19 mm, probe current = 1 nA, accelerating voltage = 20 kV and dead time = 15–30%.

Table 5 displays the main detectable elements (whose content is 1% or more) and the corresponding amounts estimated from a mean of 12 regions of interest (surface area from 20 × 13 to 210 × 140 μm^2).

The carbon contents evaluated from EDX spectroscopy are in accordance with those determined from flash combustion of the materials (Table 3), showing a higher value for C_DRAW sample.

Conversely, higher amounts of oxygen were measured here, due to preferential adsorption of oxygen on the carbon surface, which is a recognised feature of activated carbon surfaces. Some metal oxides could also be there that would not have been decomposed during (CHNS)O analysis.

The main minerals detected were calcium, silica, phosphorus and essentially iron as metal, as found previously. Corresponding values were higher than determined from the lixiviation tests but consistent in regard to relative amounts (with a much lower content for CA_DSBS than for others).

2.2.2.3. Surface chemistry. It is well-known that besides their specific surface area, the surface chemistry of adsorbents has to be considered as a key factor in their evaluation (Moreno-Castilla, 2004).

The surface acidity of adsorbents is classically evaluated from the pH at the point of zero charge (pH_{PZC}) measured by the so-called pH drift method. However, in the case of sludge-based materials the release of inorganic matter in acidic or basic media might interfere in the method and thus only a contact pH (using 0.5 g of SBCM and 50 mL of 0.1 mol L^{-1} NaCl solution prepared with deionised water) was measured.

Table 2
Textural properties of the carbonaceous materials.

Carbon	BET surface area ($m^2\ g^{-1}$)	Microporous volume ($cm^3\ g^{-1}$)	Mesoporous volume ($cm^3\ g^{-1}$)	Mean pore diameter (Å)	Structural density ρ_S ($g\ cm^{-3}$)	Porosity ε_p (–)
C_DMAD	125	0.05	0.11	44	2.60	0.29
C_DRAW	180	0.07	0.08	27	2.30	0.26
SA_DMAD	155	0.06	0.15	45	2.72	0.36
SA_DRAW	265	0.11	0.17	35	2.50	0.41
Hardened SA_DRAW	201	0.08	0.16	37	2.39	0.36
CA_DSBS	90	0.03	0.03	25	2.19	0.12
PICA F22	985	0.41	0.11	20	2.05	0.52

Table 4
Analysis of the inorganic matter of the carbonaceous materials (metal contents have been estimated from analysis of acidic leachates on the basis of original AC weight).

Carbon	Zn	Ni	Mn	Fe	Cu	Ash
			(wt%)			
C_DMAD	0.114	0.005	0.058	5.44	0.072	79.0
C_DRAW	0.026	0.002	0.012	4.37	0.058	68.5
SA_DMAD	0.119	0.031	0.064	6.21	0.069	78.2
SA_DRAW	0.061	0.003	0.015	4.79	0.067	65.0
Hardened SA_DRAW	0.066	0.003	0.016	4.97	0.073	–
CA_DSBS	0.053	0.002	0.042	0.659	0.055	59.0
PICA F22	0.001	0.002	0.001	0.058	0.003	12.0

As shown in Table 6, all carbons exhibited a basic character. Therefore the high oxygen percentage of the SBCMs is more probably tied to their inorganic part than to oxygen-containing surface groups.

3. Application of SBCMs in the AD–OX process

Following the detailed characterisation of the sludge-based materials, as described above, separate experiments were performed to evaluate their adsorption capacity and their catalytic activity in CWAO with phenol as a model pollutant. Then the behaviour of the selected SBCM was compared to that of the F22 commercial AC during five successive adsorption–oxidation cycles.

3.1. Experimental set-ups and procedures

3.1.1. Batch adsorption

Adsorption isotherms at 25 °C were measured batchwise using powdered particles sieved to a size between 200 and 400 μm to reduce equilibration time. A mass of 0.5 g of adsorbent was added to 100 mL of unbuffered phenol solution (0.005–0.05 mol L^{-1} concentration range), and the suspension was left under stirring in a thermostated bath for three days to reach equilibrium as determined by preliminary kinetic experiments. Then the solutions were filtered using 0.25 μm nylon filter membranes before analysis. The amount of adsorbed phenol was deduced from initial and final concentrations in the liquid phase; the analytical method for phenol is described in Section 3.1.4.

3.1.2. Batch oxidation

Catalytic oxidation experiments were carried out at 3.2 bar of oxygen partial pressure (total pressure of 20 bar, air and vapour) and 150 °C in a semi-batch autoclave. A mass of 2 g of carbon (0.8–1 mm sieved fraction maintained in a fixed basket) and 0.2 L of 0.05 mol L^{-1} phenol solution were mixed and left overnight for equilibration at 150 °C under a nitrogen atmosphere. Then a liquid sample was taken for initial concentration before air was provided in the reactor with a flow rate of 60 NL h^{-1} to ensure constant oxygen pressure. The stirrer speed was set to 800 rpm, enough to avoid external mass transfer resistance. Liquid samples were periodically withdrawn for analysis.

Table 5
EDX analysis of sludge-based materials (wt%).

Carbon	C	O	Mg	Al	Si	P	S	K	Ca	Fe
C_DMAD	30.8	32.3	0.6	3.9	8.8	5.1	1.0	0.3	6.9	9.7
C_DRAW	49.3	22.5	0.6	2.0	3.7	5.1	0.3	0.8	7.9	7.5
SA_DMAD	24.4	35.6	0.7	3.7	9.9	5.7	0.8	0.4	7.7	10.4
SA_DRAW	32.8	31.9	0.7	2.7	4.4	7.0	0.1	1.0	9.5	9.6
Hardened SA_DRAW	33.7	32.1	0.8	2.2	4.4	6.3	0.4	0.9	9.4	9.4
CA_DSBS	36.3	34.1	2.0	3.1	6.1	6.8	0.1	2.8	6.2	1.8

Table 6
Contact pH of the carbonaceous materials.

Carbon	Contact pH
C_DMAD	8.9
C_DRAW	8.6
SA_DMAD	9.5
SA_DRAW	8.7
CA_DSBS	8.1
PICA F22	8.8

3.1.3. AD–OX experiments

The successive adsorption–oxidation cycles were performed using a small fixed bed reactor (18 cm high and 1 cm internal diameter) to reduce the time required for bed saturation and investigate adsorbent ageing over many cycles. The schematic diagram of the set-up is shown in Fig. 1.

In this new process water purification is achieved at room temperature by adsorption on a fixed bed of activated carbon continuously fed with the polluted solution until the outlet concentration reaches the specification limit. Conversely, at the laboratory scale, the adsorption step was operated until complete bed saturation occurred, so that the adsorption capacity of fresh/regenerated carbon could be calculated from numerical integration of the breakthrough curves. Adsorption was carried out using a 0.5 g L^{-1} phenol solution at a flow rate of 0.23 L h^{-1}.

Then the storage tank connected to the reactor outlet (tank 2) was filled with 400 mL of the phenol solution circulating through the fixed bed (valve 1 on "OX" position), after which the feed was stopped. The three-way valve before the dosing pump (valve 2) was switched so that the stored solution was now used as reactor feed and thus recycled through the bed. The liquid recycling flow rate was set at 2.44 L h^{-1}.

To start the oxidative regeneration of the adsorbent, the reactor was pressurised to 50 bar with air flowing concurrently upward at 30 NL h^{-1}. Simultaneously the thermofluid circulating in the reactor jacket and in the gas–liquid preheater was heated to the required temperature. A first sample was taken in the pressurised tank when the reaction temperature of 150 °C was reached (after about 45 min). Then, as for the adsorption step, samples were periodically withdrawn for analysis (every 30 min).

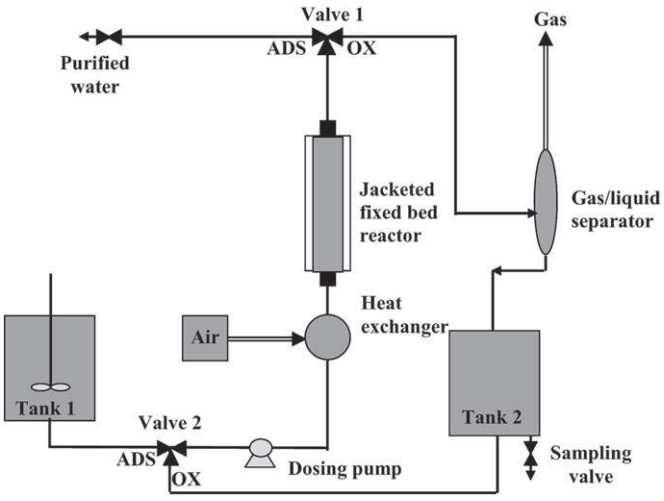

Fig. 1. Schematic diagram of the AD–OX set-up.

After 8 h of oxidation (phenol conversion in the liquid phase being 90% or more for the first cycle), the temperature of the reactor was gradually decreased from 150 °C to ambient, while maintaining gas and liquid circulation. Then the gas supply and liquid recycling were stopped, the pressure was released, and the valves switched so that another adsorption cycle could start.

3.1.4. Analytical methods

All liquid samples were analysed using a high performance liquid phase chromatograph with UV detection (UV6000 diode array detector, THERMO FINNIGAN). The separation was achieved using a C18 reverse phase column (ProntoSIL C18 AQ) with an isocratic mobile phase (40/60 mixture of acetonitrile and deionised water at pH 2.2) fed at 1 mL min^{-1}. The wavelength was set to 254 nm for phenol detection. Quantification was made from a calibration curve periodically updated with fresh standard solutions.

During oxidation, the solutions were also analysed for the remaining chemical oxygen demand (COD) according to the closed-type reflux colorimetric method using potassium dichromate as oxidant (method for 0–150 and 0–1500 mg L^{-1} ranges (Hach Company, 2003)). Precision of the method had been assessed with standard solutions and showed a standard deviation of less than 5%.

3.2. Results and discussion

3.2.1. Screening of SBCMs

3.2.1.1. Batch adsorption. Fig. 2 displays the adsorption isotherms of phenol measured at 25 °C for the different sludge-based materials and the commercial AC. F22 and SA_DRAW which have the highest BET surface area also lead to the largest phenol uptake in the investigated range of concentrations, while other SBCMs exhibit rather similar isotherms. It can be noticed that the maximum adsorption capacity of SA_DRAW is only half that of F22 while the ratio of their surface areas is nearly 1:4. The difference is more perceptible for the low phenol concentrations for which the amount adsorbed is mainly affected by the microporous volume. The incorporation of the binder appears to have more effect on the phenol uptake than expected by the change of surface area.

3.2.1.2. Batch oxidation. As explained in Section 3.1.2 a preliminary adsorption step was carried out at the reaction temperature (150 °C) before starting the CWAO. Such a procedure aims at examining separately the contributions of adsorption and oxidation to the concentration variation of the pollutant in the liquid phase as the reactor operates with low solid content. The corresponding equilibrium concentrations and respective amounts of adsorbed pollutant are given in Table 7.

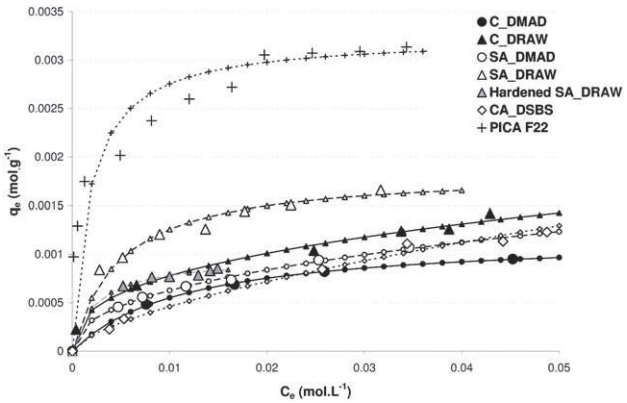

Fig. 2. Adsorption isotherms of phenol on the carbonaceous materials at 25 °C: displayed are the experimental data points (large symbols) and the isotherm plots that best fitted these points: Freundlich (C_DRAW, SA_DMAD and CA_DSBS) or Langmuir (other carbonaceous materials).

In accordance with the previous results at room temperature, SA_DRAW gave the highest phenol uptake among the sludge-based materials, which was approximately half that of the commercial carbon. As expected the adsorption capacity of the carbons at 150 °C was lower than at 25 °C (two times less on average).

Subsequently the oxidation was started by switching from nitrogen to air flow: Fig. 3 displays the evolution of normalised phenol concentration during the CWAO at 150 °C and 3.2 bar of oxygen partial pressure.

Firstly, the comparison of oxidation rates with and without the SBCMs shows a clear enhancement due to the presence of the carbons. It is especially significant with SA_DRAW which gave a higher initial oxidation rate than F22 despite its lower surface area and adsorption capacity. This may be related to its much larger amount of iron which has been proved to improve the catalytic activity of ACs (Quintanilla et al., 2006). The differences between the SBCMs are more marked when they are used as oxidation catalysts than as adsorbents and with the exception of SA_DRAW they are also ranked differently: CA_DSBS appeared to be the least efficient probably due to its relatively lower content of iron as compared to the other sludge-based materials. Hardening SA_DRAW with 5% PVA resulted in a lower catalytic activity but this was still higher than that of other SBCMs.

It can be concluded that the catalytic behaviour of the SBCMs is a complex interplay between their adsorption capacity and metal content.

Regarding the COD conversion calculated at the end of the oxidation run, the results were in agreement with the phenol conversion showing the lowest value for CA_DSBS (3.3%) and much higher ones for SA_DRAW (47.9%) and F22 (52.5%).

As was shown with commercial ACs that catalytic activity is significantly reduced when reusing the same AC sample in successive oxidations (Creanga Manole et al., 2007), deactivation has also been tested on the best SBCMs, these being SA_DRAW and hardened SA_DRAW.

Significant attrition of SA_DRAW was observed through recycling, resulting in both weight loss and decrease of particle size.

With hardened SA_DRAW unexpected features were observed, whereby almost no oxidation was evident in the first recycling run while a very fast reaction rate increase in the second recycling run occurred after a few minutes due to delayed iron leaching favouring oxidation. During the two first oxidation runs the ICP analysis of liquid samples showed negligible iron concentration in the liquid phase (less than 0.8 mg L^{-1}), while it continuously increased during the second recycling, reaching up to 120 mg L^{-1}. However it is not clear if this leaching came from the lixiviation of the starting carbonaceous material itself or from the release of micron particles due to PVA dissolution, as discrepancies were observed when

Table 7
Equilibrium concentrations and respective amounts of adsorbed phenol after preliminary adsorption at 150 °C.

Carbon	C_e (mol L^{-1})	q_e (mol g^{-1})
C_DMAD	0.043	6.0×10^{-4}
C_DRAW	0.046	4.2×10^{-4}
SA_DMAD	0.044	4.4×10^{-4}
SA_DRAW	0.041	8.6×10^{-4}
Hardened SA_DRAW	0.046	5.5×10^{-4}
CA_DSBS	0.043	6.0×10^{-4}
PICA F22	0.037	1.5×10^{-3}

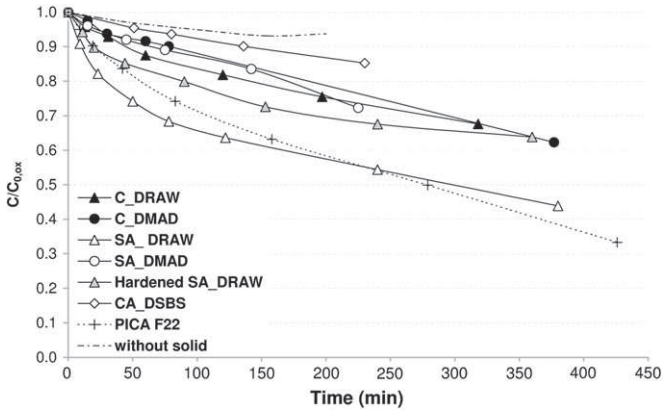

Fig. 3. Batch oxidation of phenol on the carbonaceous materials (T = 150 °C, p_{O_2} = 3.2 bar): normalised concentration–time profiles ($C_{0,ox}$ refers to the concentration after adsorption).

analysing filtered and non filtered samples. The behaviour of this composite material is further discussed in the next section.

3.2.2. AD–OX process

3.2.2.1. Preliminary runs. As SA_DRAW was not strong enough to undergo the high pressure variation of the AD–OX process (with 50 bar oxidation runs), experiments were first carried out with the hardened SA_DRAW (9.27 g, d_p = 0.8–1 mm). However, this resulted in severe foaming during the oxidation step, leading to the termination of the run and the rejection of this SBCM for the AD–OX process. Therefore only the first breakthrough curve is available for this material (Fig. 4a) and the AD–OX tests have been finally performed with one of the less efficient, but sufficiently stable carbons, C_DMAD. As stated previously its performance was compared with that of F22. The reactor was successively loaded with 10.05 g of C_DMAD (d_p = 0.8–1.6 mm) and 7.23 g of F22 (d_p = 0.8–1 mm).

3.2.2.2. Adsorption step. Fig. 4a and b displays the successive breakthrough curves measured with the SBCMs and F22 respectively.

Firstly, it can be seen that the dynamic behaviour of the commercial AC and the SBCMs are rather different, as the adsorption front is much sharper for F22 allowing nearly full saturation of the bed when the outlet concentration reaches 98% of the feed concentration; the amount of adsorbed phenol calculated from numerical integration of the breakthrough curve is 1.91×10^{-3} mol g^{-1}, while the value at equilibrium with the feed concentration (0.0053 mol L^{-1}) is 2.05×10^{-3} mol g^{-1} according to the corresponding isotherm (Fig. 2). Conversely with C_DMAD and hardened SA_DRAW only 60% of the theoretical capacity is attained when C_{outlet}/C_{feed} = 0.98 and 0.83 respectively.

Using a model that includes pore diffusion and liquid axial dispersion through a series of CSTR (Delmas et al., 2009), the effective diffusivity (D_e) can be optimised from the breakthrough curves. The following values of D_e were found to minimize the sum of squared differences between experimental and modelled concentration data: 3.47×10^{-9}, 1.85×10^{-10} and 1.28×10^{-10} m^2 s^{-1} for F22, C_DMAD and hardened SA_DRAW, respectively. Considering the value of phenol molecular diffusivity ($D_m = 1.04 \times 10^{-9}$ m^2 s^{-1}) and those of the material porosity (ε_p = 0.52, 0.29 and 0.36 respectively) it can be concluded that surface diffusion is a predominant mechanism in the case of F22 carbon, but probably not for the SBCMs (the equivalent tortuosity being 1.7 for C_DMAD and 3.0 for SA_DRAW, which are close to or within the range of usual values). Such dynamic behaviour of SBCMs is thus detrimental for their application as

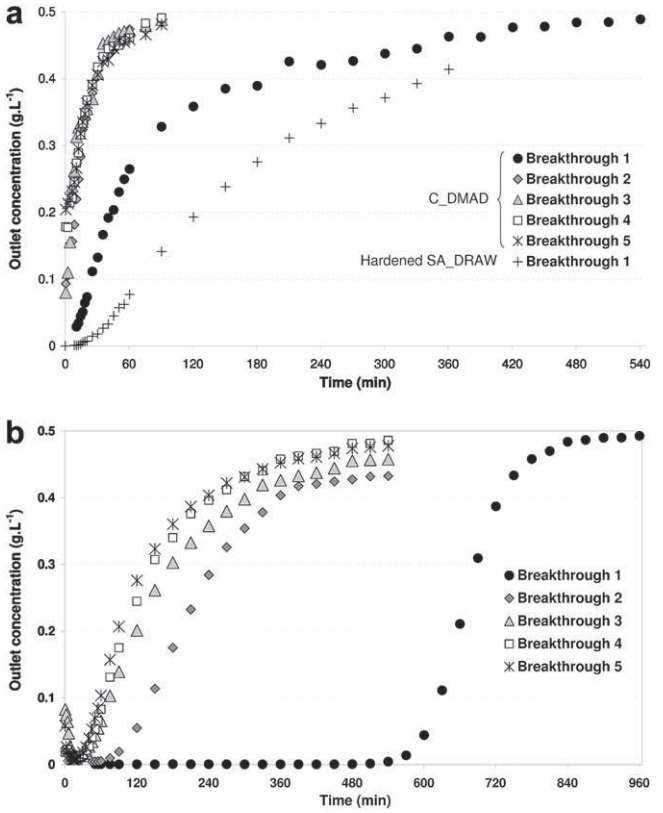

Fig. 4. Successive breakthrough curves on (a) hardened SA_DRAW (first adsorption) and C_DMAD, (b) F22: T = 25 °C, C_{feed} = 0.5 g L^{-1}, Q_L = 0.23 L h^{-1}.

adsorbents as they might lead to early breakthrough to the specification limit, well before bed saturation.

After 7 or 8 h of CWAO only a partial regeneration of the adsorptive properties of the adsorbents was achieved. The main loss is already observed at the first recycle (37.8% and 14.4% recovery for F22 and C_DMAD respectively), and then the regeneration efficiency remains nearly stable (from 28.3 to 22.7% with F22 and from 13.1 to 12.2% with C_DMAD).

Such decrease of the adsorption capacity of the commercial carbon can be related to the loss of its BET surface area (from 985 to 495 m^2 g^{-1}) and microporous volume (from 0.41 to 0.19 cm^3 g^{-1}) during the successive AD–OX cycles. This deterioration of the carbon textural properties – already reported during the oxidation of phenols – is usually attributed to the deposition of condensation products, irreversibly adsorbed and minimally oxidised, which block the access to micropores (Cordero et al., 2008). As observed for successive adsorption and oxidation runs performed in an autoclave reactor (Creanga Manole et al., 2007), this ageing occurs mainly after the first oxidation followed by quasi stable behaviour both for adsorption and oxidation (Fig. 5b).

Conversely the porosity analysis of aged C_DMAD reveals that its BET surface area remained nearly unchanged as well as its pore volume. SEM/EDX analysis of the aged carbon indicates a slightly lower carbon content (26.7%) and a higher oxygen amount (38.2%) as compared to a fresh sample (first line of Table 5). Moreover, despite a higher residual phenol concentration being obtained at the end of oxidation runs with C_DMAD as compared to F22 (Fig. 5), the remaining fraction of adsorbed phenol should not be high, because the corresponding adsorption isotherm is not very steep (as observed on Fig. 2 for fresh adsorbent at room temperature).

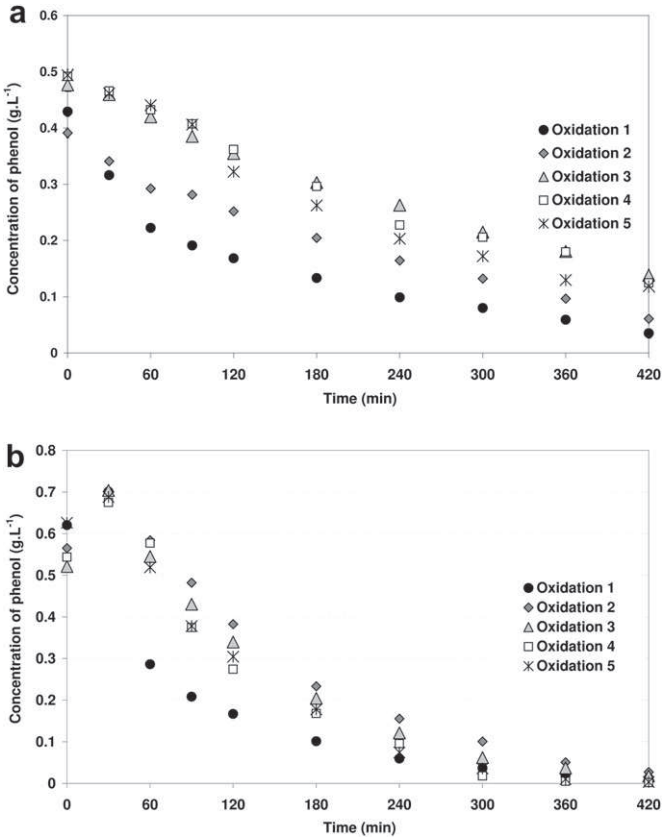

Fig. 5. Phenol concentration–time profiles measured in the recycle tank during the successive oxidations with (a) C_DMAD, (b) F22: $T = 150$ °C, $p_{O_2} = 9.5$ bar.

The decrease in the adsorption capacity of C_DMAD could therefore be due to a change of its surface chemistry.

Thus, it is believed that the commercial AC and the sludge-based material have been altered in a different manner, mainly regarding the textural properties for F22 and chemical characteristics for C_DMAD.

3.2.2.3. Oxidation step. Regarding the phenol concentration vs. time relationship measured during each oxidation trial, a clear peak can be observed for F22 at 30 min (Fig. 5b). This is due to the desorption of the pollutant when increasing the temperature (from 25 °C to 150 °C) which first dominates at the beginning of oxidation. With C_DMAD, such a peak is not seen due to the limited adsorption capacity of the material (Fig. 5a). In accordance with Fig. 3, a higher (initial) oxidation rate was found for F22 as compared to C_DMAD.

As seen for adsorption (Fig. 4), the principal changes to the concentration–time profiles occur between the two first cycles. After the first oxidation cycle, a pseudo-first order relationship with respect to the pollutant is found for C_DMAD when plotting the logarithm of liquid phase concentration as a function of time. This trend can be explained by an almost linear adsorption isotherm in the investigated range (as suggested in Fig. 2). The apparent rate constant after activity stabilisation is about 3 times lower than that given from the initial oxidation slope of the log of concentration vs. time plot. Thus, it can be concluded that iron leaching should not have occurred during the recycling of this carbon (contrarily to what was observed for hardened SA_DRAW). This is corroborated by SEM/EDX analysis of the aged C_DMAD, which shows unchanged iron content (10.1%).

For F22 the same conclusions can be reached when excluding the first point from the analysis: the oxidation data with aged AC can be fitted by a first order model (despite an expected less linear trend of the isotherm portion), resulting again in an apparent rate constant approximately 3 times lower than that observed at the very beginning of oxidation.

Now accounting for phenol concentration decreases in the solid phase together with the liquid phase during the reaction, this means that the true oxidation rate constant should have decreased even more. Thus the catalytic properties of F22 would have decreased more than its phenol adsorption capacity.

Phenol conversion in the liquid phase calculated between 30 and 420 min reached about 98% with F22 (Fig. 5b), while within the same time interval COD conversion varied from 85 (oxidation 1) to 77% showing that most of the pollutant was oxidised to carbon dioxide and water as previously found (cf. Section 3.2.1.2.). For C_DMAD the mineralization yield was less as COD conversion varied from 71% (oxidation 1) to 53% (oxidation 3) within the same time interval.

4. Conclusion

Carbonaceous materials have been synthesised from municipal WWTP sludges according to different procedures (with and without physical activation) and investigated for their physico-chemical properties and use as adsorbents and oxidation catalysts.

Their adsorption capacity for phenol – higher than expected from their BET surface area – can suggest an economically attractive utilisation of sludge-based materials as adsorbents in waste water treatment. However, their breakthrough curves indicate very slow adsorption kinetics and consequently low liquid flow rates will be required to achieve a high degree of column utilisation.

Such materials would probably not warrant regeneration, especially as the recovery yield of their adsorptive properties achieved by CWAO appears to be much less than for the reference commercial carbon.

Another potential use of SBCMs is as catalysts for continuous CWAO processes due to their naturally high iron content, but prior improvement of mechanical strength is needed for the most efficient SBCMs and long term oxidation trial runs under a range of operating conditions will be necessary.

Acknowledgements

The authors wish to acknowledge the financial support of the EU REMOVALS STREP project (http://www.etseq.urv.es/removals/index.html) under the FP6 Global Change and Ecosystems priority, contract number 018525.

They also thank PICA (Veolia group) for supplying F22 AC, Jean-Louis Labat, Ignace Coghe, Lahcen Farhi, Frank Dunglas and Lucien Pollini (LGC Toulouse) for the design and implementation of the CWAO and AD–OX experimental set-ups, Christine Rey-Rouch, Serge Mouysset, Marie-Line de Solan and Martine Auriol (SAP, LGC Toulouse) for the characterisation of the carbonaceous materials.

References

ASTM D2866, 1995. Standard Test Method for Total Ash Content of Activated Carbon. In: Annual Book of ASTM standards, 15.01, pp. 478–479.

Barrett, E.P., Joyner, L.G., Halenda, P.P., 1951. The determination of pore volume and area distributions in porous substances. J. Am. Chem. Soc. 73, 373–380.

Brunauer, S., Emmett, P.H., Teller, E., 1938. Adsorption of gases in multimolecular layers. J. Am. Chem. Soc. 60, 309–319.

Cordero, T., Rodriguez-Mirasol, J., Bedia, J., Gomis, S., Yustos, P., Garcia-Ochoa, F., Santos, A., 2008. Activated carbon as catalyst in wet oxidation of phenol: effect of the oxidation reaction on the catalyst properties and stability. Appl. Catal. B 81, 122–131.

Creanga Manole, C., Ayral, C., Julcour-Lebigue, C., Wilhelm, A.M., Delmas, H., 2007. Catalytic wet air oxidation of aqueous organic mixtures. Int. J. Chem. React. Eng. 5, A65. http://www.bepress.com/ijcre/vol5/A65.

Delmas, H., Wilhelm, A.M., Polaert, I., Fabregat, A., Stüber, F., Font, J., 2002. Sequential process of adsorption and catalytic oxidation on activated carbon for (pre)treatment of water polluted by non-biodegradable organic products. Fr. patent FRXXBL FR. A1 20021227.

Delmas, H., Creanga, C., Julcour-Lebigue, C., Wilhelm, A.M., 2009. AD–OX: a sequential oxidative process for water treatment- adsorption and batch CWAO regeneration of activated carbon. Chem. Eng. J. 152, 189–194.

European Commission, 2010. http://ec.europa.eu/environment/waste/sludge/index.htm.

Fan, X., Zhang, X., 2008. Adsorption properties of activated carbon from sewage sludge to alkaline-black. Mater. Lett. 62 (10–11), 1704–1706.

Fortuny, A., Font, J., Fabregat, A., 1998. Wet air oxidation of phenol using active carbon as catalyst. Appl. Catal. B 19 (3–4), 165–173.

Hach Company, 2003. DR/2500 Spectrophotometer procedure Manual, fourth ed.. In: Oxygen Demand, Chemical: Reactor Digestion Method.

Horvath, G., Kawazoe, K.J., 1983. Method for the calculation of effective pore size distribution in molecular sieve carbon. Chem. Eng. Jpn. 16, 470–475.

Karacan, F., Ozden, U., Karacan, S., 2007. Optimization of manufacturing conditions for activated carbon from Turkish lignite by chemical activation using response surface methodology. Appl. Thermal Eng. 27 (7), 1212–1218.

Martin, M.J., Artola, A., Balaguer, Ma.D., Rigola, M., 2002. Towards waste minimisation in WWTP: activated carbon from biological sludge and its application in liquid phase adsorption. J. Chem. Tech. Biotech. 77 (7), 825–833.

Matatov-Meytal, Y.I., Sheintuch, M., 1997. Abatement of pollutants by adsorption and oxidative catalytic regeneration. Ind. Eng. Chem. Res. 36 (10), 4374–4380.

Moreno-Castilla, C., 2004. Adsorption of organic molecules from aqueous solutions on carbon materials. Carbon 42 (1), 83–94.

Otero, M., Rozada, F., Calvo, L.F., García, A.I., Morán, A., 2003. Elimination of organic water pollutants using adsorbents obtained from sewage sludge. Dyes Pigm. 57 (1), 55–65.

Pullket, S., Smith, K.M., Fowler, G.D., Graham, N.J.D., 2009. Influence of source and treatment method on the properties of activated carbons produced from sewage sludge. J. Residuals Sci. Tech. 6 (1), 43–49.

Quintanilla, A., Casas, J.A., Zazo, J.A., Mohedano, A.F., Rodriguez, J.J., 2006. Wet air oxidation of phenol at mild conditions with a Fe/activated carbon catalyst. Appl. Catal. B 62, 115–120.

Rio, S., Faur-Brasquet, C., Le Coq, L., Le Cloirec, P., 2005. Structure characterization and adsorption properties of pyrolyzed sewage sludge. Environ. Sci. Technol. 39 (11), 4249–4257.

Rozada, F., Otero, M., Garcia, A.I., Moran, A., 2007. Application in fixed-bed systems of adsorbents obtained from sewage sludge and discarded tyres. Dyes Pigm. 72 (1), 47–56.

Santos, A., Yustos, P., Cordero, T., Gomis, S., Rodriguez, S., Garcia-Ochoa, F., 2005. Catalytic wet air oxidation of phenol on active carbon: stability, phenol conversion and mineralization. Catal. Today 102–103, 213–218.

Seredych, M., Bandosz, T.J., 2006. Removal of copper on composite sewage sludge/industrial sludge-based adsorbents: the role of surface chemistry. J. Colloid Interface Sci. 302 (2), 379–388.

Smith, K.M., Fowler, G.D., Pullket, S., Graham, N.J.D., 2009. Sewage sludge-based adsorbents: a review of their production, properties and use in water treatment applications. Water Res. 43 (10), 2569–2594.

Suarez-Ojeda, M.E., Stüber, F., Fortuny, A., Fabregat, A., Carrera, J., Font, J., 2005. Catalytic wet air oxidation of substituted phenols using active carbon catalyst. Appl. Catal. B 58 (1–2), 105–114.